Computation of the Linear Viscoelastic Relaxation Spectrum from Experimental Data

D. H. S. RAMKUMAR,[1] J. M. CARUTHERS,[1] H. MAVRIDIS,[2] R. SHROFF[2]

[1] School of Chemical Engineering, Purdue University, West Lafayette, Indiana 47907

[2] Millennium Petrochemicals, Inc., Allen Research Center, Cincinnati, Ohio 45249

Received 23 May 1996; accepted 11 September 1996

ABSTRACT: Accurate and reliable determination of the linear viscoelastic relaxation spectrum is a critical step in the application of any constitutive equation. The experimental data used to determine the relaxation spectrum always include noise and are over a limited time or frequency range, both of which can affect the determination of the spectrum. Regularization with quadratic programming has been used to derive the spectrum; however, because both the experimental data and the spectrum change by more than an order of magnitude, the input data and the spectrum are normalized in order for the numerical procedure to be accurate. Accurate determination of the relaxation spectrum requires that the spectrum extend about two logarithmic decades on either side of the frequency range of the input data. The spectrum calculated from G'' alone is more accurate at shorter relaxation times, while that from G' data alone is more accurate at longer relaxation times. Therefore, for best results, the spectrum is obtained from a combination of G' and G'' data, blended in the manner described herein. Comparison with existing methods in the literature shows a consistently improved performance of the present method illustrated with both model as well as experimental data. © 1997 John Wiley & Sons, Inc. J Appl Polym Sci **64:** 2177–2189, 1997

Key words: relaxation spectrum; regularization; linear viscoelastic data

INTRODUCTION

Determination of the relaxation spectrum is an important step in the application of any linear or nonlinear viscoelastic constitutive equation. The relaxation spectrum can, in principle, be determined from any of a number of experimentally measurable linear viscoelastic material properties; all other linear viscoelastic properties can then be determined from the spectrum.[1] However, there are several significant difficulties when this seemingly straightforward procedure is applied to actual experimental data. The topic of computing the relaxation spectrum from experimental data has attracted a lot of attention recently.[2–9] Recently Orbey and Dealy[10] have compared three methods (namely, linear regression,[2] with and without regularization,[5] and nonlinear regression[3]) to determine the discrete relaxation spectrum. They found that with the regularization method the back-calculated dynamic moduli are in better agreement with the experimental data than with the other two methods. The objective of this article is to show that the most accurate relaxation spectrum is obtained by scaling of the spectrum in the regularization scheme, by extending the spectrum about two logarithmic decades on either side of the frequency range of the

Correspondence to: R. Shroff.

Contract grant sponsor: Millennium Petrochemicals, Inc.

input data, and by using a blended function of G' and G'' data to minimize the error in regenerating the original experimental data. These objectives are further elaborated below.

The linear viscoelastic material properties [e.g., the shear modulus, $G(t)$; the dynamic shear moduli, $G'(\omega)$; and $G''(\omega)$, the dynamic viscosity $\eta'(\omega)$ and $\eta''(\omega)$, etc.] are related to the relaxation spectrum $H(\lambda)$ by a Fredholm integral of the first kind,[1] where the kernel function depends upon the linear viscoelastic material property of interest. For example, for shear modulus $G(t)$ and dynamic moduli $G'(\omega)$ and $G''(\omega)$, the relations are

$$G(t) = \int_{-\infty}^{\infty} H(\lambda)\exp(-t/\lambda)\, d\, \log \lambda \quad (1a)$$

$$G'(\omega) = \int_{-\infty}^{\infty} H(\lambda)\, \frac{\omega^2\lambda^2}{1 + \omega^2\lambda^2}\, d\, \log \lambda \quad (1b)$$

$$G''(\omega) = \int_{-\infty}^{\infty} H(\lambda)\, \frac{\omega\lambda}{1 + \omega^2\lambda^2}\, d\, \log \lambda \quad (1c)$$

Also, the kernel functions for the zero shear rate viscosity η_0, the stress decay coefficient η^-, and the stress growth coefficient η^+ are given respectively by λ, $\lambda \exp(-t/\lambda)$ and $\lambda[1 - \exp(-t/\lambda)]$.

The discrete form of the relaxation spectra can, in principle, be calculated from any of these experimental functions by discretizing the appropriate Fredholm integral. Specifically, the discretized form of eq. (1) is given by

$$G(t_i) = \sum_{\text{all } j} \exp(-t_i/\lambda_j)G_j \quad (2a)$$

where the discrete spectrum G_j is determined from the continuous spectrum $H(\lambda)$ by

$$G_j = \int_{\log\lambda_j - 1/2\Delta}^{\log\lambda_j + 1/2\Delta} H(\lambda)\, d\, \log \lambda \quad (2b)$$

and Δ is the spacing between discretized spectrum on the log λ axis. Similar results can be developed for $G'(\omega)$, $G''(\omega)$, etc., by using the appropriate kernel functions described above. The G_j spectra in eq. (2a) can be solved in principle via the traditional least-squares method, where the G_js are chosen so that the error between the experimentally measured and the predicted values of $G(t_i)$ is minimized. However, the least-squares method produces spectra with considerable oscillations, even though $G(t_i)$ is well described. This problem occurs because the kernel function matrix in eq. (2a) is inherently ill-conditioned; consequently, small errors in the input data will produce large errors in the solution spectra. These oscillations may be suppressed by large spacings between the relaxation times; however, the spectra will then lose their resolution.[5]

Regularization with quadratic programming (RQP) has been employed to minimize the oscillations in the solution of ill-posed Fredholm integral equations.[11,12] Briefly, regularization imposes a smoothness constraint on the objective function, where one minimizes the linear combination of (1) the regularization function that measures smoothness of the solution, and (2) the least-squares error between the predicted and measured input function. Lee and colleagues,[13] Honerkamp,[14] and Honerkamp and Weese[5] have applied the regularization method for determining the linear viscoelastic relaxation spectra. Honerkamp showed how ambiguities arise because of the experimental noise and incompleteness of the data.[14] A partial remedy to avoid these ambiguities was to take into account asymptotic quantities such as the zero shear viscosity and plateau modulus as shown recently by Mead.[9] However, it is often impossible to determine these quantities experimentally. One objective of this article is to use the RQP method for incomplete data but without requiring experimental determination of such asymptotic quantities.

Another concern with the straightforward application of the RQP method without the use of scaling is that both the input data and the spectra can change by orders of magnitude; consequently, very small local errors when the input data and/or the spectra are large can be much more significant to the total error than large relative errors when the input data and/or spectra are small. Therefore, a second objective is to show how the RQP method should be modified by applying suitable scaling to the solution spectra.

The third objective of this article is to examine the adverse effect of choosing the spectral width to be the inverse of the experimental frequency range as is commonly employed in the literature. Finally, although the spectrum can be determined in principle for any experimentally measurable linear viscoelastic property, different properties will be more sensitive to different regions of the spectra. For example, the kernel function of $\eta^-(t)$ (i.e., $\lambda e^{-t/\lambda}$) will emphasize the long relaxation-time part of the spectrum as compared with the kernel function of $G(t)$ (i.e., $e^{-t/\lambda}$). In this spirit, we will show how to modify the minimization cri-

terion to employ the G' data at low frequencies and the G'' data at high frequencies. Experimental difficulties in obtaining reliable transient data at both short and long times precludes accurate determination of the spectrum from transient data alone. Hence, the present work focuses on determining the spectrum from experimental dynamic data (frequency response).

The rest of this article is organized as follows: First, a brief description of the RQP method is presented in the Regularization with Quadratic Programming Method section. The Numerical Simulations section presents a critical analysis of the RQP method using model "data," where the input data is of finite extent and contains experimental noise. In this section we develop the necessary modifications to the straightforward RQP method in order to determine the relaxation spectra. In the Relaxation Spectra for IUPAC A section, the improved RQP methods are applied to the standard IUPAC A polyethylene. Finally, in the Discussion section, the significance of these results is examined. A comparison of the present method with others in the literature for computing relaxation spectra appears in the Appendix.

REGULARIZATION WITH QUADRATIC PROGRAMMING METHOD

This section briefly reviews the basic RQP method in order to provide a basis for the subsequent modifications. RQP is a method for solving the ill-posed integral equation

$$\psi(x) = \int_a^b A(x, y) f(y)\, dy \qquad (3)$$

where $A(x,y)$ is the kernel function of the integral equation, $\psi(x)$ is the experimentally measured property, and $f(y)$ is the function to be determined (i.e., the relaxation spectrum). The ill-posedness of eq. (3) exists for the kernel functions such as those in eqs. (1a)–(1c) because multiple solutions exist.[11,12] In the RQP method the functional

$$M^n[f(y); \psi(x)] = N[f(y); \psi(x)] + \Omega^n[f(y)] \qquad (4)$$

is minimized, where the least-squares error between the input data $\Psi_{\text{in}}(x)$ and the recalculation of the input data $\Psi_{\text{calc}}(x)$ using eq. (3) is given by

$$N[f(y); \psi(x)] = \int_a^b \left[\frac{\psi_{\text{cal}}(x) - \psi_{\text{in}}(x)}{\psi_{\text{in}}(x)}\right]^2 dx = \int_a^b \left[\frac{\int_a^b A(x, y) f(y)\, dy - \psi_{\text{in}}(x)}{\psi_{\text{in}}(x)}\right]^2 dx \qquad (5)$$

and the regularization function Ω^n is given by

$$\Omega^n[f(y)] = \alpha_n \int_a^b \left[\frac{d^n f(y)}{dy^n}\right]^2 dy \qquad (6)$$

where α_n is the regularization parameter. The regularization function penalizes rapid changes in the function $f(y)$, since the derivative will be large if $f(y)$ fluctuates rapidly. The regularization parameter α_n determines the relative importance given to minimizing the error between the calculated and input $\Psi(x)$ data relative to obtaining a smooth function $f(y)$. Operationally, α_n is increased systematically until the least-squares error determined by $N[f(y); \Psi(x)]$ is of the same order as the error inherent in the experimental data.

Equation (4) can be solved using standard quadratic programming methods,[15] where the derivatives in eq. (6) are approximated by simple finite differences and the integrals in eqs. (5) and (6) are approximated by the appropriate discrete summations. We will solve eq. (4) using the complementary pivot method developed by Lemke[16] via the algorithm of Ravindran and Lee.[17]

NUMERICAL SIMULATIONS

Model Spectrum and Data

In order to evaluate the effectiveness of the RQP method we need to construct a model spectrum that is completely known but is similar in form to a real viscoelastic material. The model spectrum used in this communication, shown in Figure 1, was determined from G'' data for LR723 (Quantum Chemical Co., Cincinnati, OH), which is a high-density polyethylene (HDPE) with a density of 0.952 g/cm^3 and a nominal high-load melt index (21,600 g load and 190°C) of 9.5. The G' and G'' data were determined using a Rheometrics RDA2 at 190°C. The relaxation spectra over a very limited log λ_i range were determined from the G'' data using the second order approximate method

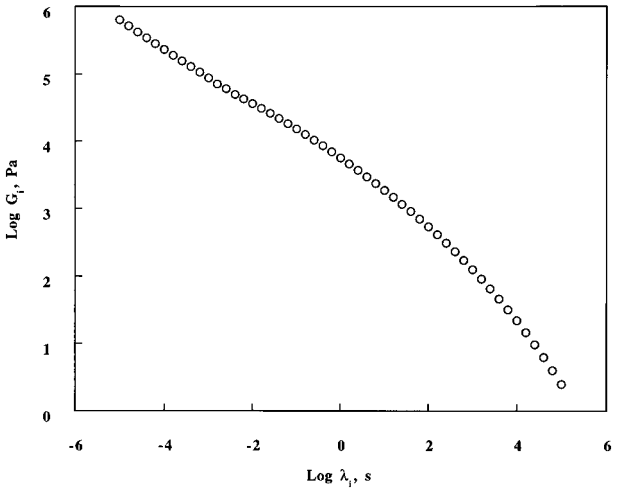

Figure 1 Model relaxation spectrum generated by extrapolating the spectrum from G'' data of LR723.

of Schwarzl and Staverman.[18] The model spectra were constructed by extrapolating the spectra determined from the G'' data to both longer and shorter relaxation times. There are five spectral points per logarithmic decade and the spectra were set to zero at λ_is less than 10^{-5} and greater than 10^5 seconds. The same spectral spacing was used throughout this work.

$G'(\omega)$ and $G''(\omega)$ model "data" have been generated from the model spectra. Experimental error has been simulated by $G' = G'_{\text{exact}}[1 + E]$, where G'_{exact} was determined from the model spectra and E is a gaussian distributed random variable with a standard deviation of 1%. Note that the experimental error is on a relative rather than an absolute basis, which is experimentally most reasonable. The dynamic viscoelastic data were generated for frequencies between 10^{-2} to 10^{+3} s^{-1} with 5 points/decade, which is nearly the largest frequency range that can be achieved for polymer melts even using time–temperature superposition. $G(t)$, $\eta^-(t)$, and $\eta^+(t)$ were generated using similar methods. We now have a set of truncated and noisy model data from which the relaxation spectrum can be determined by the RQP method.

Scaling the Spectra

The relaxation spectra have been determined by using the G' and G'' data simultaneously. Specifically, the least-squares error [i.e., N in eq. (4)] is given by

$$\begin{bmatrix} \vdots \\ G'(\omega_i) \\ \vdots \\ G''(\omega_i) \\ \vdots \end{bmatrix} = \begin{bmatrix} \cdots \dfrac{\omega_i^2\tau_j^2}{1+\omega_i^2\tau_j^2} \cdots \\ \cdots \dfrac{\omega_i\tau_j}{1+\omega_i^2\tau_j^2} \cdots \end{bmatrix} \begin{bmatrix} \vdots \\ G_j \\ \vdots \end{bmatrix} \quad (7)$$

where the second derivative regularization function is employed. In Figure 2(a) the assumed width of spectra was from 10^{-3} to 10^{+2} s, which is consistent with the $G'(\omega)$ and $G''(\omega)$ data range from 10^{-2} to 10^{+3} s^{-1}, and in Figure 2(b) the assumed spectral width was 10^{-5} to 10^{+5} s. Examination of the spectra determined without

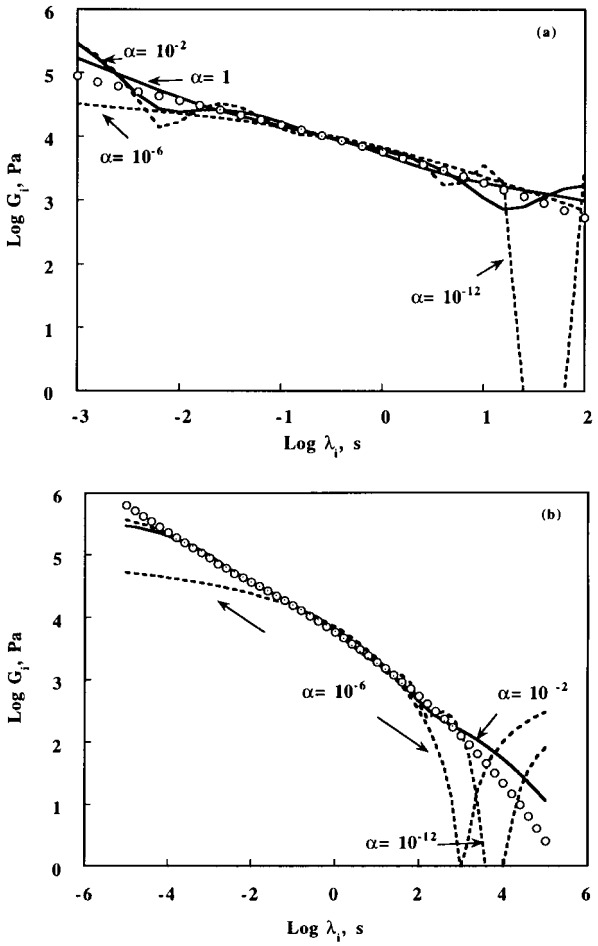

Figure 2 Effect of scaling and spectral width on the relaxation spectrum computed using the RQP method. Spectra: between (a) 10^{-3} and 10^{+2} s, and (b) 10^{-5} and 10^{+5} s. Open circles indicate model spectra, solid lines indicate scaling of the spectral strength, and dashed lines indicate the absence of scaling. Values of regularization parameter α are indicated on figure.

scaling revealed significant differences between the spectra determined via the RQP method and the input model spectra. For the narrow log λ window, the spectra are only accurately recalculated for less than one logarithmic decade. For the wider log λ window the calculated spectra are better but still do not accurately predict the model spectra, especially at longer λ_is. Since relaxation times that are just outside the experimentally measured log ω range can still contribute, it is arbitrary to truncate the spectra prematurely at the experimental log ω window. This is because the contributions for relaxation times that are two decades outside the range of the experimental frequency window are quite significant, as discussed below under the Spectral Width heading.

Examining the predictions without scaling in Figure 2(b), we observed that increasing the regularization parameter improves the predictions at shorter relaxation times at the expense of the fit at longer relaxation times. This occurs because the regularization term in eq. (6) is linear in G_i; thus, fluctuations in the spectra at large G_is (i.e., short times) are several orders of magnitude more important than fluctuations when the G_is are small (i.e., long times). It would be more realistic if the regularization could be performed with respect to log G_i instead of G_i, since it is fluctuations on a log G_i versus log λ_i plot that are most relevant. However, it is not possible to implement a nonlinear logarithmic term in the quadratic programming algorithm. It could be for the same reasons that Honerkamp and Weese[6] proposed a nonlinear regularization method to circumvent the problems associated with their linear regularization method. As an alternative, we propose scaling the G_i in order to normalize the computed spectral values to approximately unity. Specifically, each element in the $\{G_i\}$ vector in eq. (7) will be divided by $G_{i,\text{scale}}$ and the appropriate elements in the kernel matrix in eq. (7) will be multiplied by $G_{i,\text{scale}}$. Specifically,

$$\frac{\psi(x)_{\text{calc}}}{\psi(x)_{\text{in}}} = \frac{1}{\psi(x)_{\text{in}}} \sum G_{i,\text{scale}} A(x, y_i) \frac{G_i}{G_{i,\text{scale}}} \quad (8)$$

and the regularization term is given by

$$\Omega^n[f(y)] = \alpha \Sigma \left[\frac{d^2 G_i / G_{i,\text{scale}}}{d(\log \lambda_i)^2} \right]^2 \quad (9)$$

Thus the basic structure of eq. (7) is unaltered; however, the regularization function will now not unduly emphasize the large G_is. The real spectra can be recovered after application of the RQP method by multiplication by the known $G_{i,\text{scale}}$.

Any of the simple approximations for determining the spectrum from G' and G'' data can be employed for determining $G_{i,\text{scale}}$. We have used the second approximation to the spectra from $G''(\omega)$ due to Schwarzl and Staverman[18]:

$$H(\tau) = \frac{2}{\pi} \left[G'' - \frac{d^2 G''}{d(\ln \omega)^2} \right]_{1/\omega=\tau} \quad (10)$$

and the approximation for $G'(\omega)$ data by Tschoegl[19]:

$$H(\tau) = G' \left[\frac{d \log G'}{d \log \omega} - \frac{1}{2} \left(\frac{d \log G'}{d \log \omega} \right)^2 - \frac{1}{4.606} \frac{d^2 \log G'}{d(\log \omega)^2} \right]_{1/\omega=\tau/\sqrt{2}} \quad (11)$$

The scaled values for the spectrum beyond the range corresponding to the inverse of the data's frequency window have been obtained via a polynomial extrapolation of the dynamic moduli. The $G_{i,\text{scale}}$ at short times has been determined via an extrapolation of the $G''(\omega)$ data and the $G_{i,\text{scale}}$ at long time has been determined via an extrapolation of the $G'(\omega)$.

Reexamining Figure 2(b), the computed spectra are now smooth at both short and long relaxation times. The values of α are typically higher with the scaled problem because the magnitude of the curvature is reduced in comparison with the least-squares part of the objective function in eq. (4).

Input Data Set

In the studies described above, the $G'(\omega)$ and $G''(\omega)$ data were used simultaneously to determine the G_i spectra. It should be possible, in principle, to employ any of the viscoelastic material functions to determine the relaxation spectra. The effect of employing different input data is shown in Figure 3, where the spectral width in the RQP method was assumed to be between 10^{-5} and 10^{+5} s. The relaxation spectra determined from the $G''(\omega)$ data alone show excellent agreement at short times but significant deviations at long relaxation times. In contrast, the relaxation spectra determined from the $G'(\omega)$ data show excellent

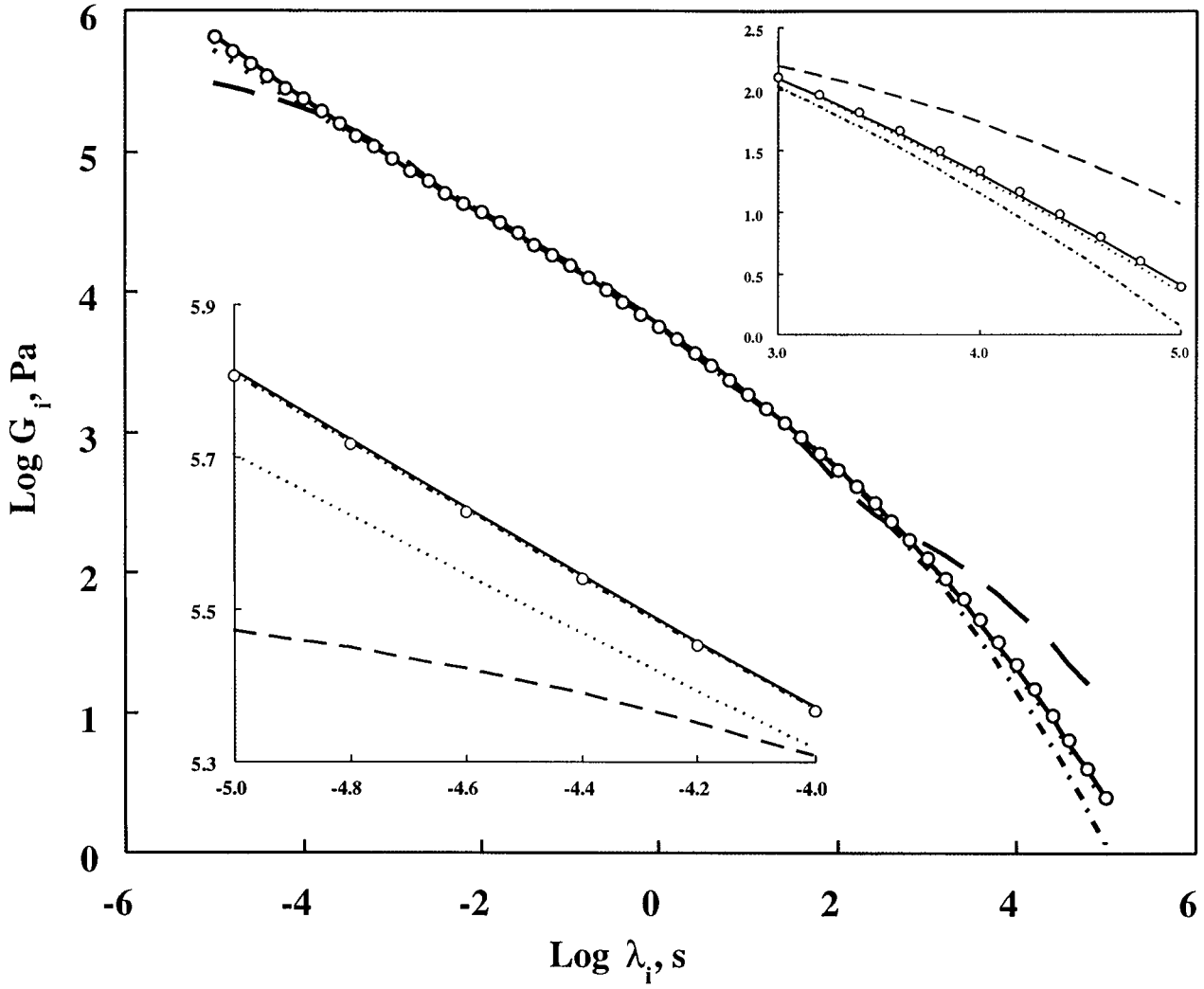

Figure 3 Effects of different input data for determining the relaxation spectra via the RQP method. Open circles indicate model spectra. Relaxation spectra calculated with: G' data, dotted line; G'' data, dot-dashed line; G' and G'' data, long dashed line; and fG' and $(1 - f)G''$, solid line.

agreement at long times but are significantly lower than the actual spectra at short relaxation times. And when the sets of $G'(\omega)$ and $G''(\omega)$ data are employed simultaneously [as defined in eq. (7)], discrepancies are observed at both long and short relaxation times.

The above observation relates to a fundamental point of this article. In Figure 4 the kernel functions of G' and G'' are shown as functions of the relaxation time λ. Referring to this figure, the following observations can be made:

1. At all frequencies the G' kernel function is nearly a step function at $\lambda = \omega^{-1}$ and consequently relaxation times shorter than ω^{-1} contribute little if any to $G'(\omega)$. Thus the storage modulus $G'(\omega)$ is dominated by the spectral contributions at long relaxation times (i.e., $\lambda > \omega^{-1}$).
2. At all frequencies the G'' kernel function is approximately bell-shaped around $\lambda = \omega^{-1}$. Thus the loss modulus $G''(\omega)$ is dominated by contribution from relaxation times around ω^{-1}, and spectral contributions from relaxation times much longer than ω^{-1} will have a negligible effect on $G''(\omega)$. The kernel function also decays rapidly for relaxation times much shorter than ω^{-1}; however, this decay is mediated because the magnitude of the relaxation spectra is

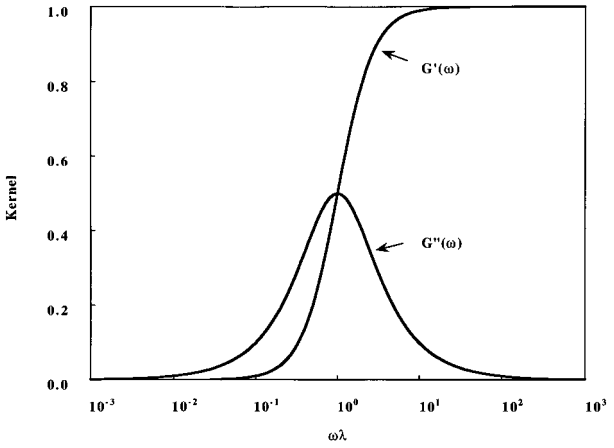

Figure 4 G' and G'' kernel functions.

generally larger at shorter relaxation times (at least in the terminal relaxation region relevant for polymer melts). Therefore, $G''(\omega)$ will be dominated by spectral contributions at short relaxation times (i.e., $\lambda < \omega^{-1}$).

Consequently, the relaxation spectrum at short relaxation times is most sensitive to high-frequency $G''(\omega)$ data and the relaxation spectrum at long relaxation times is most sensitive to low-frequency $G'(\omega)$. Determining the relaxation spectrum from $G''(\omega)$ data alone is expected to be accurate at short relaxation times, while using $G'(\omega)$ alone should provide an accurate determination of long relaxation time parts of the spectrum. This conclusion is born out by the calculated spectra in Figure 3.

The above observations not only explain why the determination of the spectrum from $G'(\omega)$ data is different from the spectrum determined using $G''(\omega)$ data, but also provide the natural remedy. The spectrum should be computed from a combination of $G'(\omega)$ and $G''(\omega)$ data blended in an appropriate manner, taking advantage of the $G'(\omega)$ sensitivity to longer relaxation times and the sensitivity of $G''(\omega)$ to shorter relaxation times. We thus propose the following objective function to be minimized:

$$M = \sum f_i \left[\frac{G'_{\text{cal}}}{G'_{\text{in}}} - 1 \right]^2 + \sum (1 - f_i) \left[\frac{G''_{\text{cal}}}{G''_{\text{in}}} - 1 \right]^2 + \alpha \sum \left[\frac{d^2(G_i/G_{i,\text{scale}})}{d(\log \lambda_i)^2} \right] \quad (12a)$$

where the blending function f_i is given by

$$f_i = 1 \Big/ \left[1 + \exp\left\{ c \ln\left(\frac{\omega_i}{\omega_f} \right) \right\} \right] \quad (12b)$$

and c is a constant. The blending function changes from emphasizing $G'(\omega)$ data to $G''(\omega)$ data at a characteristic frequency ω_f, which should be selected to be near the center of the spectrum. For this study $\omega_f = 1$. The spectrum obtained using the blending function is also shown in Figure 3. The agreement of the computed spectrum with the model spectrum is now excellent at both short and long relaxation times. The effect of the constant c in the blending function on the computed spectra is shown in Figure 5. If c is greater than or equal to 1, excellent agreement is observed between the predicted and model spectrum. We will use $c = 5$ throughout the remainder of this work.

Spectral Width

As shown in Figure 2(a), if the spectrum is computed over a range of relaxation times corresponding to the inverse of the frequency window there will be significant errors in the prediction of the spectrum. Examining the form of the $G'(\omega)$ and $G''(\omega)$ kernel functions, contributions from relaxation times that are two logarithmic decades outside the range of the experimental frequency window can be significant. The effect of the assumed spectral width on the relaxation spectra determined by RQP is shown in Figure 6. If the spectral width is not extended beyond the range of the experimental data, significant errors occur. A slight discrepancy is observed when the assumed

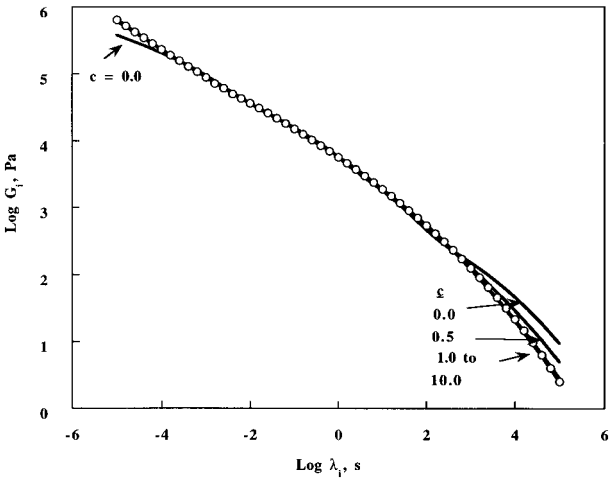

Figure 5 Effect of the constant c in the blending function on the computed relaxation spectra.

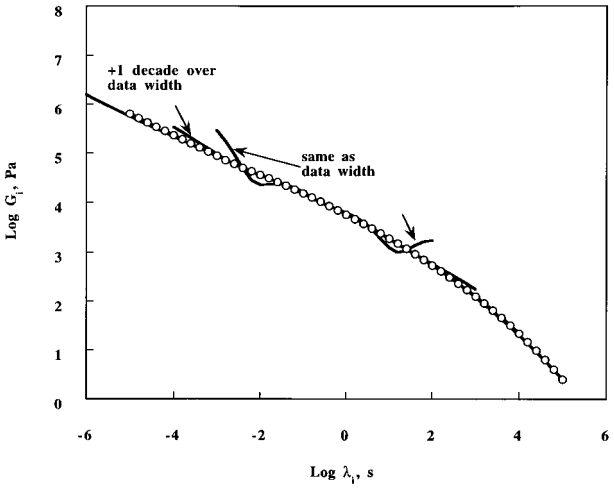

Figure 6 Effect of spectral width on the computed relaxation spectra. Spectral widths of ±2 and ±3 logarithmic decades greater are the solid line that lies upon the model spectra indicated by the open circles.

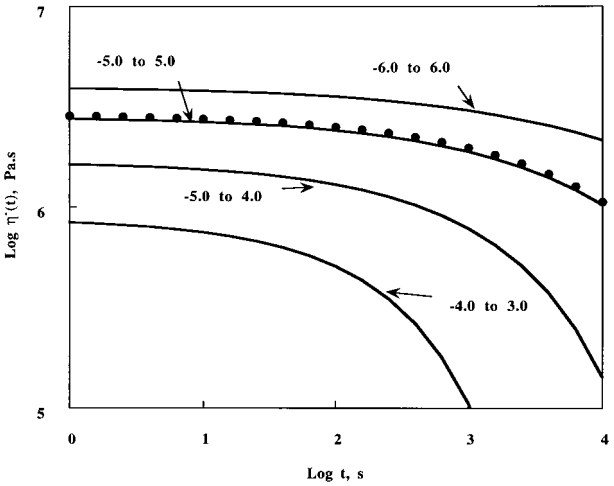

Figure 7 Effect of spectral width on the stress relaxation function $\eta^-(t)$. Open circles indicate response computed from the model spectra. The assumed range of log λ_i is indicated in the figure.

spectral width is extended only one logarithmic decade beyond the experimental frequency range. However, when the log λ window is extended two or more logarithmic decades on either side of the experimental log ω window, the computed spectra are identical to the actual spectrum.

Prediction of Other Linear Viscoelastic Material Functions

The spectra recomputed via the modified RQP method accurately describe the $G'(\omega)$ and $G''(\omega)$; this is hardly surprising, however, since the M^n function in eq. (4) is designed to minimize the error between the input and recomputed $G'(\omega)$ and $G''(\omega)$ data. A more critical test is to compute the spectra from one set of linear viscoelastic data and recompute a different viscoelastic response. Using the RQP method with $G'(\omega)$ and $G''(\omega)$ input data, the $G(t)$ response was computed and the predicted response was identical to the $G(t)$ response determined using the model spectra. The predicted responses for the stress decay coefficient $\eta^-(t)$ and stress growth function $\eta^+(t)$ are shown respectively in Figures 7 and 8. These transient responses are very sensitive to the assumed spectral width that was used in the RQP procedure, even though the input and recalculated $G'(\omega)$ and $G''(\omega)$ agreed over the log ω range of the input data for all the assumed spectral widths. The discrepancies at short times in the predicted $\eta^-(t)$ response occur because of errors in determining the zero shear rate viscosity η_0. Specifically, η_0 is an integral over all relaxation times, and thus truncation errors severely affect the prediction of η_0. Thus the modified RQP method does accurately extend the spectra outside the experimental log ω range; however, abrupt truncation of the spectra well outside the experimental log ω window cannot be determined reliably. The abrupt truncation of the spectra is primarily an artifact of this model viscoelastic material because it is highly unlikely that the viscoelastic processes in any real material would exhibit an abrupt cutoff.

If reliable transient data are available, they

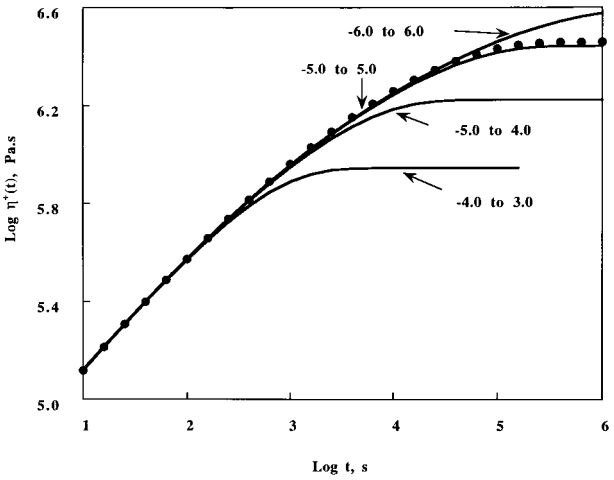

Figure 8 Effect of spectral width on the stress relaxation function $\eta^+(t)$. Open circles indicate response computed from the model spectra. The assumed range of log λ_i is indicated in the figure.

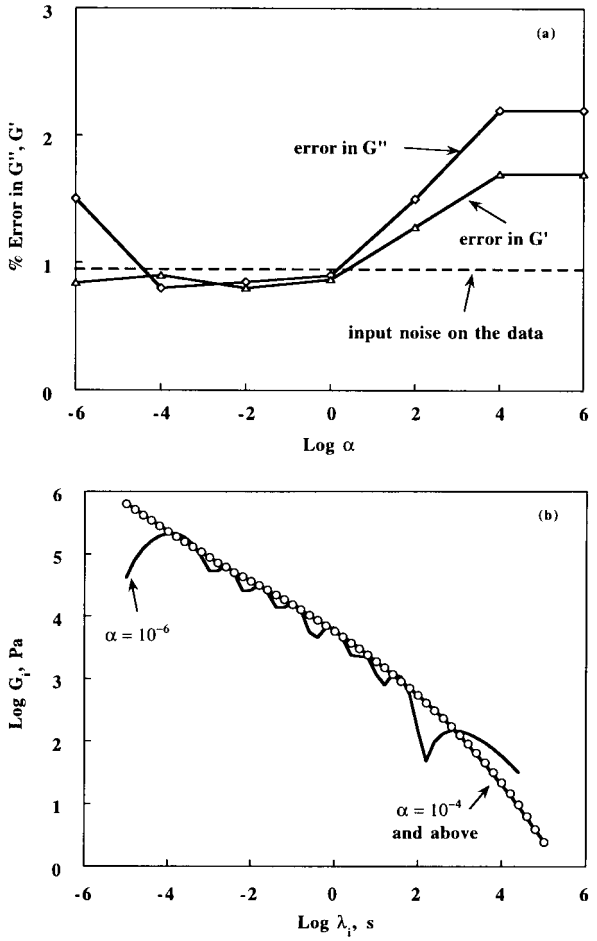

Figure 9 Effect of the regularization parameter on the $G'(\omega)$ and $G''(\omega)$ error (a) and the relaxation spectrum (b).

can be used effectively to assess the necessary spectral width. Alternatively, the transient data could be employed as input data along with the dynamic data. The major drawback to this scheme is that instrument artifacts often plague $\eta^-(t)$ and $\eta^+(t)$ data. The present method is not limited to the oscillatory data; one just needs to include the right kernels in eq. (7).

Regularization Parameter

The final RQP-method variable that must be assessed is the regularization parameter α. The effects of α on the error in G', G'', and G_i spectra are shown in Figure 9, where the blending function was employed and the log λ range was -5 to $+5$. The G' error reported in Figure 9(a) was computed as follows:

$$G' \text{ error} = \left[\frac{1}{m-1}\sum_m (G'_{\text{in}} - G'_{\text{calc}})^2\right]^{1/2} \quad (13)$$

where m is the number of data points. The G'' error is computed in a similar manner. At low values of α the G' and G'' errors are relatively insensitive to the regularization parameter; however, when α exceeded 10° the error in both G' and G'' increased dramatically because curvature in the relaxation spectra was over-penalized by the regularization term. For log α less than 0 the relative error in both G' and G'' was approximately 1%, which was the magnitude of the random noise added to the model data. This is reasonable because the calculated solution should not fit the input data better than the inherent noise in the data. Examining Figure 9(b), at log α of -6, the calculated spectrum is oscillatory; however for log α of -4 and larger, smooth spectra are obtained. Thus a log α of -2 or -1 is optimum because it will provide the smoothest spectrum while ensuring consistency with the error in the back-calculated G' and G'' responses.

Comparison with Other Methods

A comparison of the present method with other methods in the literature for computing relaxation spectra appears in the Appendix. The comparison is performed using both model spectra and experimental data from the literature. The excellent performance of the method of the present work is illustrated in Figures A.1 and A.2, and demonstrated quantitatively in Table A.I.

RELAXATION SPECTRA FOR IUPAC A

In this section the regularization procedures developed in the previous section are applied to IUPAC A polyethylene. The spectra were obtained using $G'(\omega)$ and $G''(\omega)$ data of Zosel[20] which were available from a log ω of -2 to $+2$. The relaxation spectra were computed for log λ_i between -4 and $+4$, which is a two-decade extrapolation on either side of the data's frequency range. The blending function [eq. (12b)] with $c = 5$ was used and the optimum log α was determined to be -1. The relaxation spectrum is tabulated in Table I and shown graphically in Figure 10.

The relaxation spectrum previously determined by Laun[2] using the traditional least-squares approach is also shown in Figure 10. The

Table I Relaxation Spectrum of IUPAC A Determined Using the Present Method

$\log \lambda_i$ (s)	$\log G_i$ (Pa)
−4.0	4.796
−3.8	4.723
−3.6	4.651
−3.4	4.581
−3.2	4.512
−3.0	4.443
−2.8	4.375
−2.6	4.307
−2.4	4.239
−2.2	4.170
−2.0	4.099
−1.8	4.027
−1.6	3.952
−1.4	3.875
−1.2	3.795
−1.0	3.714
−0.8	3.633
−0.6	3.552
−0.4	3.472
−0.2	3.389
0.0	3.287
0.2	3.170
0.4	3.053
0.6	2.923
0.8	2.777
1.0	2.614
1.2	2.433
1.4	2.235
1.6	2.021
1.8	1.789
2.0	1.540
2.2	1.271
2.4	0.982
2.6	0.672
2.8	0.339
3.0	−0.017
3.2	−0.398
3.4	−0.806
3.6	−1.241
3.8	−1.705
4.0	−2.199

spectrum determined by Laun is shifted vertically from the spectrum determined via the modified RQP method. This is a consequence of the wider spectral spacings employed by Laun to prevent unrealistic oscillations that can occur in an unconstrained least-squares procedure. There is some difference in shape at both short and long relaxation times, some of which is due to changes in the spectral spacing in Laun's spectrum at long relaxation times, but there are also some real differences. The differences in the two spectra are shown in Figure 11 for the prediction of the normalized stress growth function $\eta^+(t)/\eta_0$, where η_0 is the zero-shear-rate viscosity. The spectrum determined via the modified RQP method seems to provide a somewhat better fit to the experimental $\eta^+(t)$ data, probably because the RQP method does a better job of determining the spectra at relaxation times just longer than the experimental frequency window.

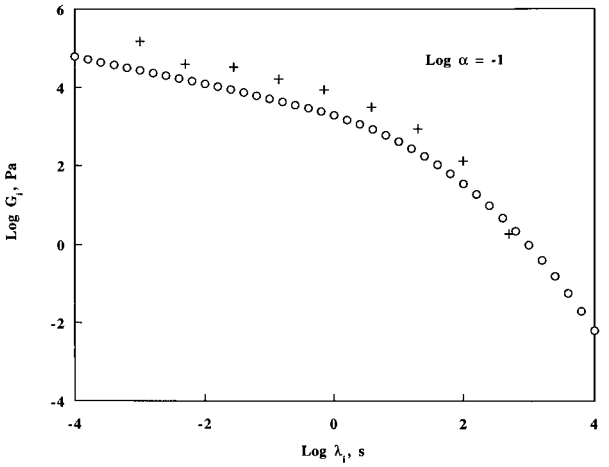

Figure 10 Relaxation spectrum for IUPAC A. Open circles indicate spectral strengths given in Table I. Pluses are spectral values of Laun.[2]

DISCUSSION

In order to determine the relaxation spectrum accurately from dynamic linear viscoelastic data,

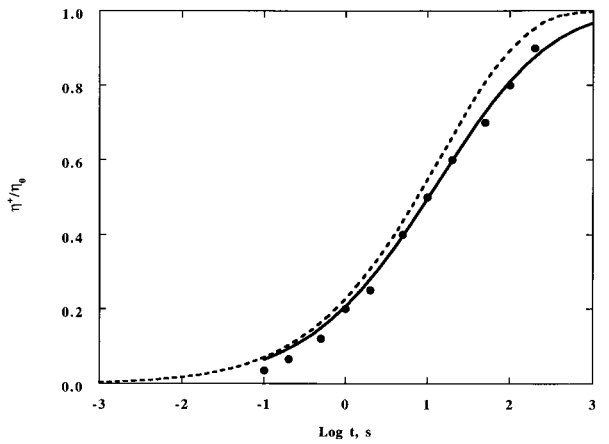

Figure 11 Stress growth function for IUPAC A. Solid points indicate experimental data. Solid line is computed from the spectrum given in Table I; dashed line is computed from the spectrum of Laun.[2]

the RQP procedure should be modified. Specifically, the assumed spectral width must be at least two logarithmic decades wider than the experimental data, the spectral strengths in the regularization term [i.e., eq. (9)] must be scaled appropriately, and the least-squares error should emphasize the $G'(\omega)$ data at low frequencies and the $G''(\omega)$ data at high frequencies. Although these modifications are not revolutionary, they are nevertheless essential in order to determine the relaxation spectrum accurately.

It is interesting to note that the spectrum can be determined at relaxation times outside the range of the experimental data. In fact, the modified RQP method is stable for as large a spectral width as one wants to employ; however, the significance of the spectrum well outside the data range must be considered carefully. Specifically, spectral contributions that lie within the range of the input data obviously contribute to G'_{calc} and G''_{calc} in the minimization function given by eq. (12a); and spectral contributions that are outside the data range but close to the input data (e.g., ± 1.5 logarithmic decades outside the log ω range) will still effect G'_{calc} and G''_{calc}, although to a lesser extent. Spectral contributions well outside the range of the experimental data (e.g., more than two logarithmic decades outside the frequency window) will not contribute to the least-squares-error part of the minimization function; however, changes in the spectra well outside the data range will contribute to the regularization part of the minimization function. Since the second derivative of the spectra is used in the minimization function, changes in the slope of the spectra at very short and very long relaxation times will be penalized. Thus the modified RQP method will essentially effect a smooth extrapolation of the spectra for relaxation times well outside the frequency range of the experimental data.

This article's emphasis on the accurate determination of the relaxation spectrum raises the obvious question of whether the differences between the various methods are significant. We address this question with the following example: Figure 12 shows the relaxation spectra determined from dynamic data at 150°C for two low-density polyethylene (LDPE) resins, where differences in the relaxation spectra are observed at long relaxation times. LDPE-B is a shear modified version of LDPE-A that occurs after a single pass through an extruder. LDPE-A is a 0.46 Melt Index, 0.9334 density, 7.9% vinyl acetate, LDPE resin in pellet form. The optical properties were measured on 1.5-mil blown film produced from the two resins. LDPE-A had a haze level of 33 while LDPE-B had a haze level of 24 (i.e., LDPE-B shows a 27% improvement over LDPE-A). The improvement in optical properties is in accord with past studies which show that optical properties improve with reduction in LDPE melt elasticity.[21,22] It is also known that shear modification of LDPE reduces melt elasticity.[23] The shear modification is also suspected to be responsible for the different behaviors of LDPE resins IUPAC A, B, and C.

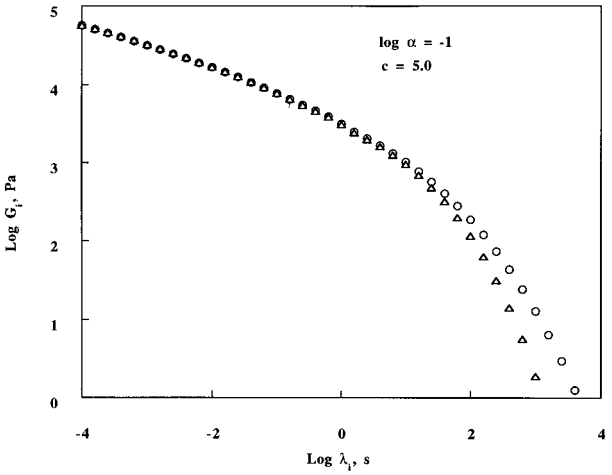

Figure 12 Relaxation spectra for two polyethylene materials. Open circles indicate unmodified material and triangles indicate a shear-modified material.

Returning to Figure 12 it can be observed that LDPE-A has a broader relaxation spectrum at long times and therefore has a higher melt elasticity, which explain its poorer optical properties. However, the difference in the two spectra becomes apparent only at relaxation times greater than 10^2 s, which are outside the experimental frequency window of log $\omega = -1.6$ to 2.6 rad/s. Thus the ability to infer differences in the spectra is made possible only by using a method that is sensitive enough to accurately and reliably resolve the differences between LDPE-A and LDPE-B at relaxation times that are outside the range of the experimental data.

One of the authors (D.H.S.R.) was supported by a generous research grant from the Millennium Petrochemicals, Inc., Cincinnati, Ohio.

Table A.I Average Absolute Deviation (AAD) for Dynamic Moduli Back-Calculated with Discrete Spectra Obtained by Different Methods[10]

Sample	Method	AAD in G'	AAD in G''
Model data of Honerkamp and Weese[5]	Present work	0.028	0.045
	Honerkamp and Weese[5]	3.00	4.10
	Baumgaertel and Winter[3]	5.12	5.35
	Laun[2]	6.98	10.16
Polybutadiene	Present work	0.018	0.011
	Honerkamp and Weese[5]	0.76	0.94
	Baumgaertel and Winter[3]	1.18	1.26
	Laun[2]	16.6	13.7
HDPE	Present work	0.041	0.020
	Honerkamp and Weese[5]	0.85	1.26
	Baumgaertel and Winter[3]	1.33	1.12
	Laun[2]	4.82	2.73

$$\text{AAD} = \frac{1}{M}\sum_{i=1}^{M} \left| \left(G'_{\text{exp}} - G'_{\text{cal}} \right) / G'_{\text{exp}} \right| .$$

APPENDIX: COMPARISON OF RELAXATION SPECTRA CALCULATED WITH DIFFERENT METHODS

Different Model Spectra

Model Spectrum of Honerkamp and Weese[5]

The spectrum is a bimodal distribution; the data range is log ω: -3 to 3 with 4% random error. The relaxation spectrum was calculated with the present RQP method using the following parameters: log λ: -5 to 4; log α: -3, 5 points/decade, c (the parameter in the blending function) = 5.

Figure A.1 compares results of the present work with the original model spectrum. This figure also contains the spectra calculated by Orbey and Dealy[10] with the methods of (1) Honerkamp and Weese,[5] (2) Baumgaertel and Winter,[3] and (3) Laun.[2] The spectral points of the other methods were read out from Figure 1 of Orbey and Dealy.[10] The parameter h_0 in Figure A.1 is defined as

$$h_0 = \ln(\lambda_b/\lambda_a)/(N-1) \qquad \text{(A.1)}$$

In eq. (A.1), N is the total number of spectral points, and λ_a and λ_b refer to the lower and upper bounds, respectively, of the relaxation time range. The absolute average deviations (AAD) in G',G'' from different methods are given in Table A.I. The spectrum computed with the present method cap-

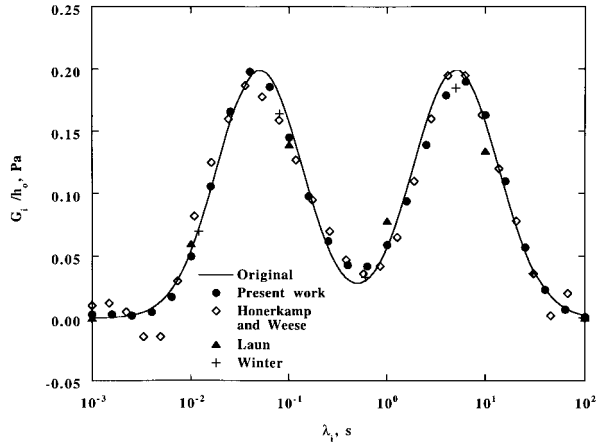

Figure A.1 Model relaxation spectrum of Honerkamp and Weese.[5]

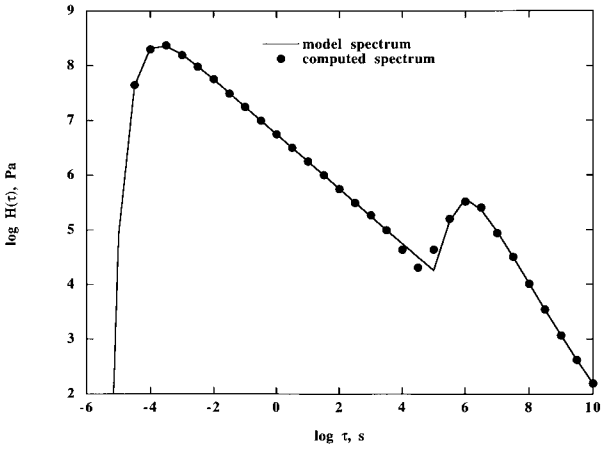

Figure A.2 Model relaxation spectrum of Emri and Tschoegl.[7]

tures all the important features of the original spectrum. Additionally, the present method predicts the end regions very well compared with the other methods shown. The AADs in G'',G' are also lower with the present method.

Model Spectrum of Emri and Tschoegl[7,8]

This model spectrum is an asymmetric bimodal distribution with the range log λ: -5.5 to 10.0. Their data range for the master curve is log ω: -10 to 10. Figure A.2 compares the continuous spectrum obtained by the present method (log λ: -5.5 to 10.0; log α: -4.0, 2 points/decade, $c = 5$) with the model continuous spectrum.

Experimental Data

Polybutadiene Melt

The dynamic data for this melt in the range log ω: 0.397 to 3.047 have been given by Honerkamp and Weese.[5] The parameters used in the RQP method of the present work are: log λ: -5 to 1; log α: -4, 5 points/decade, $c = 5$.

HDPE Melt

The dynamic data range from log ω: -2 to 2. The parameters used are: log λ: -4 to 3; log α: -2, 5 points/decade, $c = 5$. The AADs in G',G'' obtained with the present method on these melts also appear in Table A.I. In both cases, the results of the present method show superior accuracy over the other methods.

REFERENCES

1. J. D. Ferry, *Viscoelastic Properties of Polymers,* Wiley, New York, 1980.
2. H. M. Laun, *J. Rheol.,* **30,** 459 (1986).
3. M. Baumgaertel and H. H. Winter, *Rheol. Acta,* **28,** 511 (1989).
4. V. M. Kamath and M. R. Mackley, *J. Non-Newt. Fluid Mech.,* **32,** 119 (1989).
5. J. Honerkamp and J. Weese, *Macromolecules,* **22,** 4372 (1989).
6. J. Honerkamp and J. Weese, *Rheol. Acta,* **32,** 65 (1993).
7. I. Emri and N. W. Tschoegl, *Rheol. Acta,* **32,** 311 (1993).
8. I. Emri and N. W. Tschoegl, *Rheol. Acta,* **32,** 322 (1993).
9. D. W. Mead, *J. Rheol.,* **38,** 1769 (1994).
10. N. Orbey and J. M. Dealy, *J. Rheol.,* **35,** 1035 (1991).
11. V. A. Morozov, *Methods of Solving Incorrectly Posed Problems,* Springer, New York, 1984.
12. M. Bertero, *Inverse Problems,* A. Dold and B. Eckmann, eds., Springer, Berlin, 1986.
13. C. Y.-C. Lee, D. R. Wiff, and V. G. Rodgers, *J. Macromol. Sci.-Phys.,* **B19**(2), 211 (1981).
14. J. Honerkamp, *Rheol. Acta,* **28,** 363 (1989).
15. G. V. Reklaitis, A. Ravindran, and K. M. Ragsdell, *Engineering Optimization—Methods and Applications,* Wiley, New York, 1983, pp. 480–494.
16. C. E. Lemke, *Manage. Sci.,* **11,** 681 (1965).
17. A. Ravindran and H. Lee, *Eur. J. Opr. Res.,* **8,** 166 (1981).
18. F. Schwarzl and A. J. Staverman, *Appl. Sci. Res.,* **A4,** 127 (1953).
19. N. W. Tschoegl, *The Phenomenological Theory of Linear Viscoelastic Behavior,* Springer, Berlin, 1989.
20. J. Meissner, *Pure Appl. Chem.,* **42,** 551 (1975).
21. M. Shida, R. N. Shroff, and L. V. Cancio, *Polym. Eng. Sci.,* **17,** 769 (1977).
22. M. S. Pucci and R. N. Shroff, *Polym. Eng. Sci.,* **26,** 569 (1986).
23. M. Rokudai, *J. Appl. Polym. Sci.,* **23,** 463 (1979).